Impulse noise detection and removal using fuzzy techniques

D. Zhang and Z. Wang

Indexing terms: Image enhancement, Noise measurement, Fuzzy systems

A new algorithm is presented which can remove impulse noise from corrupted images while preserving details. The algorithm is based on fuzzy impulse detection and fuzzy noise cancellation techniques. Experimental results show that the algorithm is capable of providing significant improvement over many published techniques in terms of both subjective and objective evaluations.

Introduction: In recent years, fuzzy modelling and reasoning have been successfully used in various applications [1]. A typical application area using fuzzy techniques is to recover images corrupted by impulse noise [2].

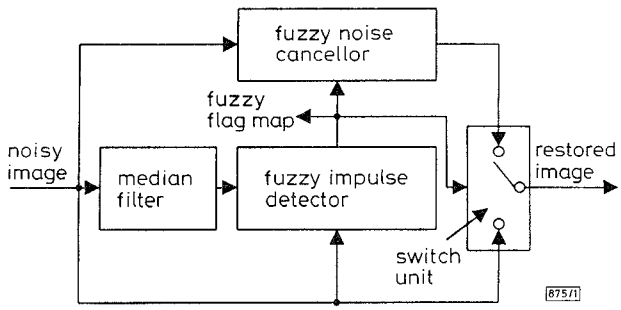

Fig. 1 *Fuzzy impulse noise removal system*

In this Letter, we present a new impulse noise removal algorithm which is shown in Fig. 1. Our algorithm starts by the input of the noisy image to a median filter. The output image of the median filter, together with the noisy image itself, is the input of our fuzzy impulse detection module. The goal of the fuzzy impulse detection module is to generate a fuzzy flag map which gives each pixel a fuzzy flag indicating how much it looks like an impulse pixel. This fuzzy flag map has two usages: (i) the fuzzy noise cancellation module utilises it to recommend a new value for every pixel; (ii) it is also used as the basis of the switch unit which controls each pixel of the output restored image in two different cases. The recommended value of the fuzzy noise cancellation module or the input pixel value remain unchanged. Finally, the output of the switch unit is our restored image.

Fuzzy impulse detection: Let $x_{i,j}$ and $y_{i,j}$ represent the pixel values at position (i, j) in the corrupted image and the restored image, respectively. To judge whether $x_{i,j}$ is an impulse pixel, we obtain the median value of the samples in the $(2N_d + 1) \times (2N_d + 1)$ window centred about it, i.e.

$$v_{i,j} = \text{med}\{x_{i-N_d,j-N_d}, \ldots, x_{i,j}, \ldots, x_{i+N_d,j+N_d}\} \quad (1)$$

The difference between $v_{i,j}$ and $x_{i,j}$ provides us with a simple and effective measure for detecting impulses: If the difference between $v_{i,j}$ and $x_{i,j}$ is large, then it is an impulse pixel. To give the pixel (i, j) a fuzzy flag indicating how much it looks like an impulse pixel, we define the following two-parameter membership function:

$$f_{i,j} = \begin{cases} 0 & |x_{i,j} - v_{i,j}| \le a \\ \frac{|x_{i,j} - v_{i,j}| - a}{b - a} & a < |x_{i,j} - v_{i,j}| < b \\ 1 & |x_{i,j} - v_{i,j}| \ge b \end{cases} \quad (2)$$

where a and b are the two pre-determined parameters. We can use $(1 - f_{i,j})$ as a measurement to demonstrate how good a pixel is.

Fuzzy noise cancellation: According to our impulse noise removal system described in Fig. 1, the noise cancellation scheme is applied only to the pixels which look like impulses, i.e. if $f_{i,j} \le T_d$, then $y_{i,j} = x_{i,j}$; Otherwise, the fuzzy noise cancellation algorithm is used to yield a new value for $y_{i,j}$ which is different from $x_{i,j}$. Here T_d is a given threshold value.

Our noise cancellation algorithm is based on a special kind of information redundancy – long range correlation within different parts of the image. For a pixel at position (i, j) to be modified, two $(2N_c + 1) \times (2N_c + 1)$ sized windows are used: the first window is defined as a local window centred about the impulse pixel; the second window is defined as a remote window located at a different place with its centre at position (k, l). Since the whole image may contain a large number of complete $(2N_c + 1) \times (2N_c + 1)$ windows, the remote window should be chosen from one of them. In our algorithm, a candidate remote window must satisfy the following conditions: (i) it must be completely covered by a larger $(2M + 1) \times (2M + 1)$ $(M > N_c)$ window called the searching range window which is centred about the impulse pixel; (ii) it is not the same as the local window, i.e. $i \neq k$ or $j \neq l$. All the $(2N_c + 1) \times (2N_c + 1)$ windows satisfying these requirements are subjected to a fuzzy window matching test. Before describing how the test is performed, however, we define a fuzzy pixel matching function based on the following fuzzy reasoning: If the difference between a pair of corresponding pixels in the local and remote windows is small, then the two pixels are well matched. The function is defined as

$$p_{m,n} = \begin{cases} (T_m - |x_{i+m,j+n} - x_{k+m,l+n}|)/T_m & |x_{i+m,j+n} - x_{k+m,l+n}| < T_m \\ 0 & |x_{i+m,j+n} - x_{k+m,l+n}| \ge T_m \end{cases} \quad (3)$$

where T_m is a pre-defined parameter. If a pair of corresponding pixels are well matched and both of the pixels are good, then the pair is a good matching pair. If most of the matching pixel pairs in the local and remote windows are good matching pairs, then the two windows are well matched. Based on the above fuzzy rules, we use the following standard to determine how well a pair of local and remote windows are matched:

$$q_{(i,j),(k,l)} = \sum_{m=-N_c}^{N_c} \sum_{n=-N_c}^{N_c} p_{m,n} \times \min[(1 - f_{i+m,j+n}), (1 - f_{k+m,l+n})](1 - \delta_{m,n}) \quad (4)$$

where

$$\delta_{m,n} = \begin{cases} 1 & m = 0 \text{ and } n = 0 \\ 0 & \text{otherwise} \end{cases} \quad (5)$$

Each of the candidate remote windows will result in $q_{(i,j),(k,l)}$, but only the window with maximum $q_{(i,j),(k,l)}$ becomes our ultimate choice. Finally, the pixel value of (i, j) is replaced by a linear com-

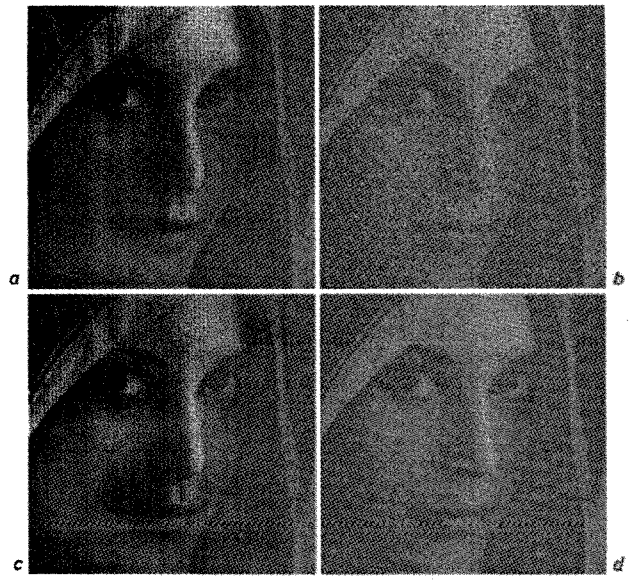

Fig. 2 *Restoration performance*

a Original face region of 'Lena'
b Corrupted image by 20% random-valued impulse noise
c After first iteration
d Restored image after second iteration

bination of its original value $x_{i,j}$ and the centre pixel $x_{k,l}$ of the selected remote window:

$$y_{i,j} = [(1 - f_{i,j})x_{i,j} + (1 - f_{k,l})x_{k,l}]/(2 - f_{i,j} - f_{k,l}) \quad (6)$$

where the linear coefficients are determined on how good $x_{i,j}$ and $x_{k,l}$ are.

Experimental results: Some computer simulations are carried out to assess the performance of our method. The original test image is 'Lena' of size 512 × 512 (8 bit/pixel). The corrupted images are generated using both fixed-valued impulse noise (equal values of 0 or 255 with equal probabilities) and random-valued impulse noise (random values uniformly distributed between 0 and 255). We use the proposed approach to remove noises from the corrupted images. Usually, the best restoration results are obtained after two or three iterations. Fig. 2 gives the restoration result for the face region of 'Lena' where the image is corrupted by 20% random valued impulse noise. The restored image appears to have a very good subjective quality.

To make a comparison with other published algorithms, the peak signal-to-noise ratio (PSNR) is used to give a quantitative evaluation. In [5], Abreu *et al.* reported many restoration results in PSNR for images corrupted by both 20% fixed-valued and 20% random-valued impulse noises. We list some of these data in Table 1 and add the result of our algorithm at the end of the Table. Clearly, the proposed algorithm outperforms all the other methods including those published in [5] which have, as far as we know, the best restoration results in the literature.

Table 1: Comparative restoration results in PSNR for 20% impulse noise for image 'Lena'

Algorithm	Fixed-valued impulses[1], dB	Random-valued impulses[2], dB
Median filter (3×3)	28.57	29.76
Median filter (5×5)	28.78	28.59
Median filter with adaptive length[3] [3]	30.57	31.18
Rank conditioned rank selection filter[4] [4]	31.36	30.78
Abreu *et al.* (M = 1296) (inside training set)[3,5] [5]	35.70	33.37
Our new fuzzy approach	36.47[6]	33.78[7]

[1] Impulses take on only values 0 or 255. [2] Impulses are uniformly distributed between 0 and 255. [3] Implemented recursively, i.e. the modified pixel values are immediately used in process of following pixels. [4] Implemented non-recursively using 9×9 window for fixed-valued impulses, and recursively using 3×3 window for random-valued impulses. M = 2 (M as defmed in [2]) [5] M as defined in [5] [6] N_d = 1, a = 24, b = 44, T_d = 0.3, N_c =2, T_m = 28, M = 15, after 3 iterations. [7] N_d = 1, a = 8, b = 28, T_d = 0.2, N_c = 2, T_m = 31, M = 12, after two iterations

Conclusions: In this Letter, we present a new impulse noise removal method by using fuzzy impulse detection and fuzzy noise cancellation algorithms. The usage of fuzzy techniques provides us with a tradeoff between considering good information as much as possible, and avoiding the influence of bad information. Experimental results indicate that the proposed method provides a significant improvement over other algorithms in terms of both subjective and objective evaluations.

8 January 1997
Electronics Letters Online No: 19970257

D. Zhang and Z. Wang (*Department of Computer Science, City University of Hong Kong, Kowloon, Hong Kong*)

References

1 JANG, J.R., SUN, C.T., and MIZUTANI, E.: 'Neuro-fuzzy and soft computing' (Prentice Hall, 1997)
2 RUSSO, F., and RAMPONI, G.: 'A fuzzy filter for images corrupted by impulse noise', *IEEE Sig. Process. Lett.*, 1996, **3**, (6), pp. 168–170
3 LIN, H.M., and WILLSON, A.N.: 'Median filters with adaptive length', *IEEE Trans. Circuits Syst.*, 1988, **35**, (6), pp. 675–690
4 HARDIE, R.C., and BARNER, K.E.: 'Rank conditioned rank selection filters for signal restoration', *IEEE Trans. Image Process.*, 1994, **3**, (2), pp. 192–206
5 ABREU, E., LIGHTSTONE, M., MITRA, S.K., and ARAKAWA, K.: 'A new efficient approach for the removal of impulse noise from highly corrupted images', *IEEE Trans. Image Process.*, 1996, **5**, (6), pp. 1012–1025

Pixelless infrared imaging device

H.C. Liu, L.B. Allard, M. Buchanan and Z.R. Wasilewski

Indexing terms: Image processing, Infrared imaging, CCD image sensors

A new concept for infrared imaging using a pixelless photon frequency up-conversion device together with a CCD array is presented. The concept is applicable to wavelengths longer than the CCD response range (longer than about 1.1μm). Preliminary imaging results using a quantum well infrared photodetector integrated with a light emitting diode are also presented.

CCDs are excellent imaging devices for the visible and near infrared (IR) (up to a wavelength of ~1.1μm) spectral regions. The ultraviolet regions and even beyond can be covered by coating a CCD with appropriate luminescent materials. For wavelengths longer than the CCD response range, an efficient and low-cost imaging device is not widely available. Arrays based on InAs are capable of covering the wavelength range shorter than ~3μm, but these devices are not well developed. For the 3–12μm wavelength IR region, arrays based on InSb or HgCdTe are commonly used, but they are costly. For even longer wavelengths (>12μm), only special purposes can justify the high cost of imaging arrays, such as for satellite based instrumentation and for astronomy use. The newly developed arrays based on quantum well infrared photodetectors (QWIPs) [1] have some cost advantages over InSb and HgCdTe, but they still require special hybrid readout circuits. Many applications could benefit from the availability of a low-cost imaging device in the spectral region longer than that of a CCD. In this Letter, we propose a novel approach for achieving this goal.

The basic idea is shown in Fig. 1. The photon frequency up-conversion device concept is shown in the upper part where either *a* a photodiode or *b* a photoconductor is connected in series with an LED. The photodiode or the photoconductor acts as the long wavelength IR detector, whereas the LED emits in the near IR or the visible spectrum falling into the CCD response range. A forward constant bias voltage (V_+) is applied to the LED with the other side of the series grounded. A long wavelength IR excitation of the detector decreases its resistance and thereby increases the voltage dropped across the LED, leading to an increase in the LED emission intensity. We have therefore converted the in-coming long wavelength IR into an increase of the visible or near IR emission. Note that for the photodiode case, instead of connecting the two *n*-type contact sides together, the two *p*-type sides can also be connected, in which case the applied voltage should be negative in polarity. Similarly, for the photoconductor case, the polarity of the LED and the bias voltage can be reversed, in which case the photoconductor should work on hole carrier conduction. One specific embodiment of a single element up-conversion device from 9μm to 930nm has been presented in [2].

The essential elements of achieving a pixelless imaging device are shown in Fig. 1*c* where a simple two-terminal mesa device on a substrate is shown. The up-conversion device is made sufficiently large in area for a long wavelength IR image, and the emitted image is detected by a CCD. The key requirements for up-converting the long wavelength IR image into the LED emission image with negligible distortion, smearing, and crosstalk are as follows: (i) the entire active part of the detector-LED structure must be thin. (the Figure is not drawn to scale: the height of the mesa is much smaller than the dimension of the device area.) In practice, due to the diffraction limit in optical elements, a thickness of less